

# NONEQUILIBRIUM EFFECTS IN THE TUNNELING CONDUCTANCE SPECTRA OF SMALL METALLIC PARTICLES

Oded Agam

The Racah Institute of Physics  
The Hebrew University  
Jerusalem, 91904  
Israel

## 1 Introduction

Trace formulae and the non-linear supersymmetric  $\sigma$ -model are basic analytical tools used successfully in the fields of quantum chaos and disordered systems. Both are designed to treat systems with a small number of degrees of freedom. Hence they are limited in their possibility of analyzing many-body systems where interparticle interactions play an important role, and the number of degrees of freedom is large.

On the other hand, many experimental studies of quantum chaos use systems which consist in a large number of interacting particles, for example quantum dots or disordered metallic particles. Having an elaborate single-particle description of these systems, it is of prominent importance to understand the role of interactions, the range of applicability of a single-particle picture, and the interplay between chaos and interparticle interactions.

In this respect, an important observation is that strong chaotic dynamics, on the level of non-interacting single-particle description, provides us with the possibility of analyzing interacting many-body systems by a systematic perturbative approach. The small parameter of this perturbation theory is  $1/g$ , where  $g = t_H/t_c$  is the dimensionless conductance, i.e. the ratio of the Heisenberg time,  $t_H$  (the inverse mean level spacing), to the classical relaxation time,  $t_c$ .

The general form of the interaction Hamiltonian in which particles interact via a two-body potential  $U(\mathbf{r}, \mathbf{r}')$  is

$$H_{\text{int}} = \frac{1}{2} \sum_{ijkl} \sum_{\sigma\sigma'} U_{ijkl} c_{i\sigma}^\dagger c_{j\sigma'}^\dagger c_{k\sigma'} c_{l\sigma}, \quad (1)$$

where  $c_{i\sigma}^\dagger$  and  $c_{i\sigma}$  are the creation and annihilation operators for a particle in state  $\psi_i$  and spin  $\sigma$ , while

$$U_{ijkl} = \int d\mathbf{r} d\mathbf{r}' U(\mathbf{r}, \mathbf{r}') \psi_i^*(\mathbf{r}) \psi_j^*(\mathbf{r}') \psi_l(\mathbf{r}) \psi_k(\mathbf{r}')$$

are the matrix elements of the interaction potential. These matrix elements can be divided into two groups according to their typical magnitude. One contains diagonal matrix elements, namely those  $U_{ijkl}$  in which two pairs of indices are identical. All the other matrix elements, which we call off-diagonal, are included in the second group. In appendix A it is shown that the typical magnitude of off-diagonal matrix elements is as small as  $d/g$  where  $d$  is the single-particle mean level spacing and  $g$  is the dimensionless conductance. The same smallness restricts also the fluctuations in the diagonal matrix elements. Therefore, the interaction Hamiltonian of electrons in a quantum dot takes the form

$$H_{\text{int}} = \frac{e^2}{2C} \left( \sum_{i\sigma} c_{i\sigma}^\dagger c_{i\sigma} - N_0 \right)^2 - \lambda \sum_{i,j} c_{i\uparrow}^\dagger c_{i\downarrow}^\dagger c_{j\uparrow} c_{j\downarrow} + \frac{a}{2} \sum_{ij,\sigma\sigma'} c_{i\sigma}^\dagger c_{j\sigma'}^\dagger c_{i\sigma'} c_{j\sigma} + O(d/g). \quad (2)$$

The first term of this formula is the orthodox model<sup>1, 2</sup> representing the charging energy of the dot:  $C$  is the total capacitance of the dot,  $N = \sum_{i\sigma} c_{i\sigma}^\dagger c_{i\sigma}$  is the total number of electrons in the dot, and  $N_0$  is a continuous parameter controlled by the gate voltage. The second term, when  $\lambda > 0$ , represents an attractive interaction which drives the grain into a superconducting state at sufficiently low temperatures and weak magnetic field. The last term represents the electron-electron interaction in the spin channel, and the coefficient  $a$  is of order the single-particle mean level spacing,  $d$ .

Strong chaotic dynamics of the noninteracting particles implies that  $g \gg 1$ . Consequently, all off-diagonal matrix elements  $U_{ijkl}$  are proportional to  $1/g$ , and the mean field approximation (2) for the interacting Hamiltonian (1) is justified. Indeed, many phenomena of normal and superconducting metallic grains are described by the approximation (2). The most prominent one is the Coulomb blockade, which is essentially the quantization of the number of electrons in the grain away from the charge degeneracy point. Because of this quantization, the zero-bias conductance of the system vanishes, while the current  $I$  as the function of the source-drain voltage  $V$  shows a threshold behavior. The fine structure of the current-voltage curve is associated with the single-electron levels of the system<sup>3, 4</sup>.

Nevertheless, there are interesting phenomena emerging from the fluctuations of the interaction matrix elements, i.e. with the  $O(d/g)$  corrections to (2). In this review we analyze two experiments of Ralph, Black and Tinkham<sup>5, 6</sup> and show that fluctuations of the interaction energy, although small as  $d/g$ , clearly manifest themselves in the differential conductance spectra of ultrasmall metallic grains. The small effects of fluctuations in the charging energy are especially pronounced due to the fact that the system is driven out of equilibrium, and is able to explore several high excited states at relatively low source-drain voltage.

The experimental system consists of a single aluminum particle connected to external leads via high resistance (1 – 5 M $\Omega$ ) tunnel junctions formed by oxidizing the surface of the particle. The device (see illustration in Fig. 1) is fabricated using electron beam lithography and reactive ion etching to form a bowl-shaped hole in an insulating Si<sub>3</sub>N<sub>4</sub> membrane. The opening at the lower edge of the membrane is 3-10 nm in diameter. Al is evaporated onto the bowl-shaped side of the membrane, and subsequently the Al surface is oxidized. The oxide layer forms a tunnel barrier in the vicinity of the small hole in the membrane. The membrane is then flipped up side down and a small amount of Al is deposited. Because of surface tension, the Al forms a layer of electrically isolated particles, a few nanometers in size. Following a second oxidation, a thick layer of Al is deposited on top of the particles.\* In approximately 25% of the

\* In other configurations of these devices a gate electrode of ring shape is deposited after flipping the membrane, and the same procedure follows the oxidation of the gate.

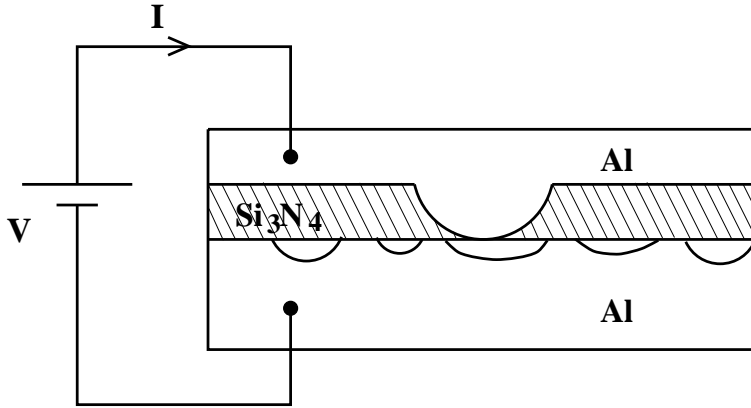


**Figure 1.** A schematic illustration of the device used in the experiments of Ralph, Black and Tinkham for measuring the differential conductance spectra of ultrasmall aluminum grains.

devices one Al particle covers the hole in the nitride membrane, so that the electrons passing between the leads tunnel through the metal particle.

The capacitances and the resistances of the tunnel junctions are estimated by fitting the large scale  $I - V$  curves,  $eV \sim e^2/C$ , to the Coulomb blockade staircase pattern. From the capacitances one can determine the area of the tunnel junctions and the volume of the grain which is used in turn to estimate the single-particle mean level spacing<sup>5</sup>.

In this review we focus our attention on scales of the  $I - V$  curves which are much smaller than that of the Coulomb blockade, scales over which the single-particle mean level spacing,  $d$ , and the fluctuation in the charging energy,  $d/g$ , are resolved. Fig. 2 displays the differential conductance,  $dI/dV$ , of two different *normal* metallic particles (of sizes roughly 2.5 and 4.5 nm) as a function of the source-drain bias energy  $eV$ . The spectra display three clear features:

1. The low resonances of the differential conductance are grouped in clusters. The distance between nearby clusters is of order the mean level spacing  $d$  of the noninteracting electrons in the dot.
2. The first cluster contains only a single resonance.
3. Higher clusters consist of several resonances spaced much more closely than  $d$ .

In section 2 it will be shown that these features are manifestations of the interplay between electron-electron interactions and nonequilibrium effects<sup>7</sup>. Each cluster of resonances is identified with one excited single-electron state, and each resonance in turn is associated with a different occupancy configuration of the metal particle's other single-electron states. The appearance of multiple resonances reflects the strongly nonequilibrium state of the particle.

In another experiment<sup>6</sup>, Ralph, Black and Tinkham measured the tunneling resonance spectra of ultrasmall *superconducting* grains. The number of electrons in the system was controlled by a gate voltage. The results of this experiment, depicted in Fig. 3, show that:

1. For the ground state of the grain with an even number of electrons, the first peak of the differential conductance is merely shifted by the gate voltage  $V_g$ . The shape of this peak does not change over a large interval of  $V_g$ . Contrarily, if the grain

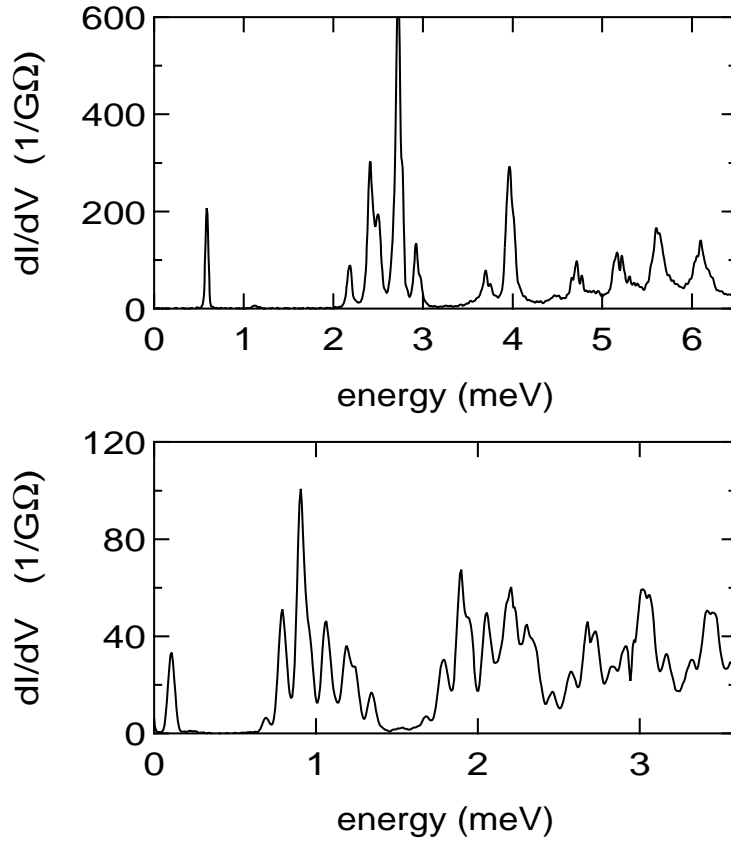


**Figure 2.** The low temperature (30 mK) differential conductance  $dI/dV$  versus bias energy of ultrasmall Al particles with volumes  $\approx 40 \text{ nm}^3$  (upper panel)  $\approx 100 \text{ nm}^3$  (lower panel). The first resonance is isolated while subsequent resonances are clustered in groups. The distance between nearby groups of resonances is approximately the single-particle mean level spacing  $d$ . (From Ref. [5]).

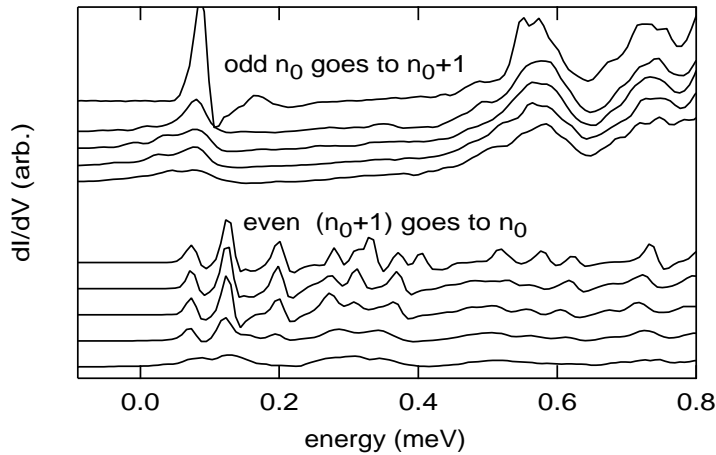


**Figure 3.** The tunneling resonances of superconducting grains in the odd (upper scans) and the even (lower scans) charging states. Different scans correspond to different value of the gate voltage, and are artificially shifted in energy to align peaks due to the same eigenstate. In contrast with Fig. 2 the first resonance, in the odd charging state, develops a substructure when shifted by the gate voltage. (From Ref. [6]).

contains an odd number of electrons, the height of the first peak rapidly reduces with a change of the gate voltage, and a structure of subresonances develops on the low-voltage shoulder of this peak.

2. The characteristic energy scale between subresonances of the first peak is of the order of the mean level spacing  $d$ .

These observations contrast the results for the normal case in which the first peak did not split. Nevertheless, it was suggested in Ref. [6] that the substructure of the first peak is still associated with nonequilibrium steady states of the grain. In section 3, the origin of these nonequilibrium states and the mechanism which generates them will be clarified<sup>8</sup>.

The explanations for both experiments discussed here rely on the assumption that the systems are stimulated into steady states which are far from equilibrium, namely that relaxation processes are too slow to maintain the system in equilibrium. In section 4 we summarize the various relaxation processes and estimate the inelastic time,  $\tau_{in}$ , for electrons in the dot. The results will be summarized in section 5.

## 2 Normal grains

Our model for the experimental system is given by the Hamiltonian:  $H = H_0 + H_T + H_{\text{int}}$ . Here  $H_0$  describes the noninteracting electrons in the left (L) and right (R) leads and in the metallic grain<sup>†</sup>,

$$H_0 = \sum_{\alpha=L,R} \sum_q \xi_{\alpha q} d_{\alpha q}^\dagger d_{\alpha q} + \sum_l \xi_l c_l^\dagger c_l. \quad (3)$$

Tunneling across the barriers is described by

$$H_T = \sum_{\alpha=L,R} \sum_{q,l} T_{ql}^{(\alpha)} d_{\alpha q}^\dagger c_l + \text{H.c.}, \quad (4)$$

where  $T_{ql}^{(\alpha)}$  are the tunneling matrix elements. Interaction effects given by (1) are taken into account only for the electrons in the grain, but including screening by image charges in the leads.

For the ultrasmall aluminum grains considered here, one can neglect superconducting pairing since the single-particle mean level spacing,  $\approx 1$  meV, is larger than the BCS superconducting gap which is 0.18 meV<sup>9</sup>. Under this condition, the interaction term of the electrons is generally approximated by the orthodox model,  $H_{\text{int}} \approx (e \sum_l c_l^\dagger c_l)^2 / C$ , where  $C$  is the effective capacitance of the grain<sup>1</sup>. Within this approximation the charging energy depends only on the total number of electrons in the dot, but not on their particular occupancy configuration. The orthodox model is able to account for the Coulomb blockade<sup>1</sup>, and the Coulomb staircase behavior of the current as the number of extra tunneling electrons in the dot increases. It can also be generalized to describe features on the scale of the single-particle level spacing<sup>10</sup>. However, the orthodox model cannot account for the clusters of resonances in Fig. 2, since these result from fluctuations,  $\delta U$ , in the interaction energy between pairs of electrons.

We focus our attention on the (experimental) voltage regime where there is no more than one extra tunneling electron in the dot. At small voltage bias,  $V$ , within the Coulomb-blockade regime [Fig. 4(a)], current does not flow through the system. Current

<sup>†</sup>Unless explicitly written, from now on single-particle and spin states will be denoted by a single subscript.

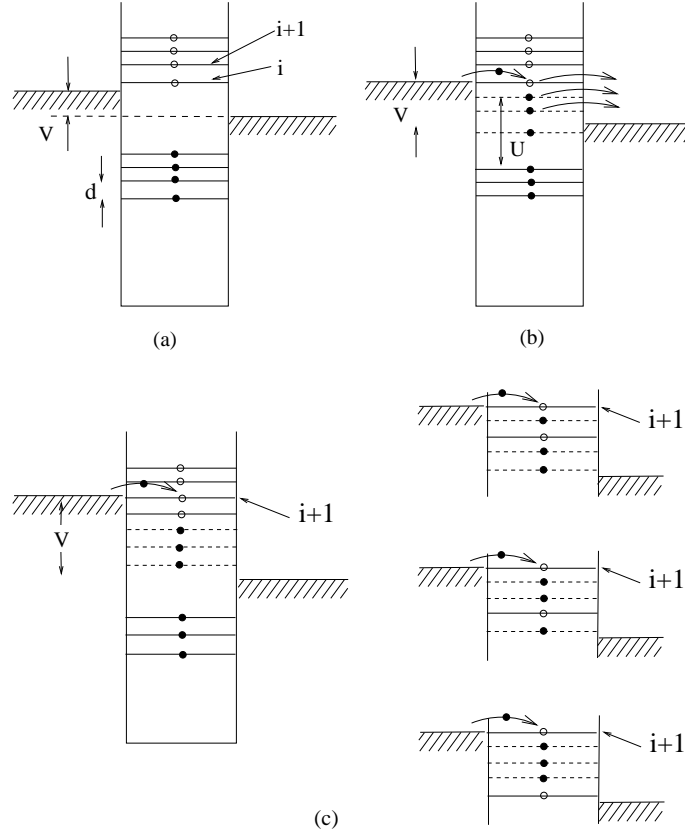


**Figure 4.** An illustration of transport through the metal particle at various values of the source–drain voltage  $V$ . Filled single-particle levels are indicated by full circles and empty ones by open circles.  $U$  is the charging energy, and  $d$  is the single-particle mean level spacing. (a) The system at small voltage bias within the Coulomb blockade regime; (b)  $V$  corresponding to the first resonance in Fig. 2. The thin dashed lines indicate the energy of a level after an electron has tunneled into the dot; (c)  $V$  near the first cluster of resonances in Fig. 2. The splitting within the first cluster originates from the sensitivity of level  $i + 1$  to the different possible occupation configurations as shown.

first starts to flow when one state  $i$  inside the grain becomes available for tunneling through the left barrier, say, as illustrated in Fig. 4(b). As the system becomes charged with an additional electron, the potential energy of the other electrons in the dot increases by  $U \simeq e^2/C$ , and some of the lower energy occupied electronic states are raised above the right lead chemical potential [in Fig. 4(b) these “ghost” states are shown as dashed lines]. Electrons can tunnel out from these states into the right lead leaving the particle in an excited state. There is, however, only one configuration of the electrons which allows an electron to tunnel into level  $i$  from the left lead, namely all lower energy levels occupied. This implies that only a single resonance peak appears in the differential conductance at the onset of the current flow through the system (broken spin degeneracy would cause splitting of this peak).

The situation changes when  $V$  increases such that electrons can tunnel from the left lead into the next higher available state  $i + 1$ , as shown in Fig.4 (c). In this case, there are several possible occupancy configurations, on which the exact energy of level  $i + 1$  depends. The several possible energies of level  $i + 1$  lead to a cluster of resonances in the differential conductance of the grain. The scenario described above holds provided that inelastic processes are too slow to maintain equilibrium in the particle.

To explicitly demonstrate the splitting of resonances induced by fixed fluctuations in the interaction energy  $\delta U$ , model detailed-balance equations<sup>10</sup> were solved numeri-

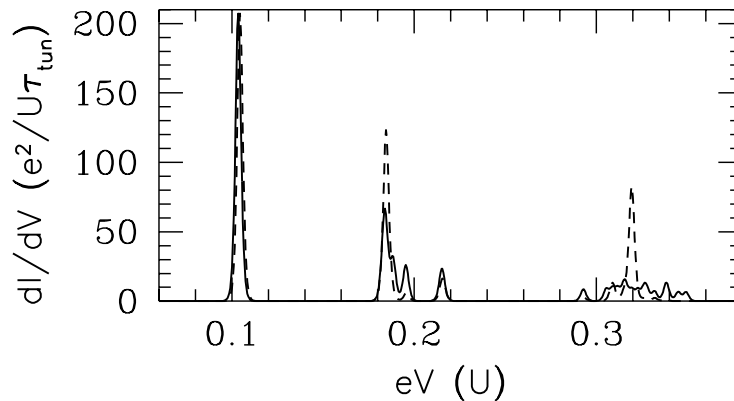


**Figure 5.** Model differential conductance obtained from nonequilibrium detailed-balance equations: solid line – in the absence of inelastic processes,  $1/\tau_{in} = 0$ ; dashed line – with inelastic relaxation rate larger than the tunneling rate,  $1/\tau_{in} = 5/\tau_{tun}$ .

cally and the corresponding differential conductance plotted in Fig. 5 by the solid line. The model system consists of 7 equally spaced levels, occupied alternately by 4 or 5 electrons, in a current-carrying steady state. For simplicity, the tunneling rate into each level,  $1/\tau_{tun}$  ( $\Gamma_{L(R)}(\epsilon_l)$  in the notation of Ref. [10]), is chosen to be uniform, and the voltage is applied by increasing the left chemical potential. The temperature is 1% of the mean level spacing  $d$ , and the variance of the fluctuations  $\delta U$  in the interaction energy is  $d/5$ . In the absence of fluctuations ( $\delta U = 0$ ),  $dI/dV$  consists of single resonances spaced by  $d$ .

To estimate the fluctuations in the interaction energy consider the Hartree term of the interaction energy,  $U_H$ . We wish to calculate the interaction energy difference associated with different occupation configurations of low energy states. Suppose that, as illustrated in Fig. 4(c), these differ by a single occupation number, namely, in one configuration the state  $j$  is empty and  $j'$  is full while in the other  $j'$  is empty and  $j$  is full. Then

$$\delta U_H = \int dr_1 dr_2 |\psi_i(\mathbf{r}_1)|^2 U(\mathbf{r}_1, \mathbf{r}_2) [|\psi_{j'}(\mathbf{r}_2)|^2 - |\psi_j(\mathbf{r}_2)|^2],$$

where the index  $i$  labels an electron state other than  $j$  or  $j'$ ,  $U(\mathbf{r}_1, \mathbf{r}_2)$  is the interaction potential. Since wave functions of chaotic systems associated with different energies are statistically independent,  $\langle \delta U_H \rangle = 0$  where  $\langle \dots \rangle$  denotes ensemble or energy averaging. We are therefore interested in fluctuations of  $\delta U_H$  which emerge from the non-uniform probability distributions of the single-particle eigenstates in real space. The calculation of  $\langle \delta U_H^2 \rangle$  is similar to that presented in appendix A. The result for diffusive systems is

$$\langle \delta U_H^2 \rangle = \left( c \frac{d}{g} \right)^2,$$

where  $c = \sqrt{2}\alpha \sum_{\mathbf{n}} |\mathbf{n}|^{-4} / \pi$  is a constant of order unity, and  $\alpha$  equals two for system with time reversal symmetry and unity for systems without time reversal symmetry<sup>‡</sup>. The above estimate for the fluctuations in the charging energy also applies for

<sup>‡</sup>This estimation does not take into account a change in the potential due to the insertion of an additional electron. It was argued that the latter effect may lead to an even stronger effect, i.e.  $\delta U \sim d/\sqrt{g}$ .<sup>11</sup>

general chaotic systems, with  $g = \hbar\gamma_1/d$  where  $\gamma_1$  is the first non-vanishing Perron-Frobenius eigenvalue<sup>12</sup>, see appendix A.

The increase of the fluctuations in the interaction energy as  $g$  decreases is related to the fact that  $g$  is a measure for the uniformity of the single-particle wave functions. The bigger  $g$  the more uniform are the wave functions and the less are the fluctuations in the interaction energy. Experimentally we find  $g \approx 5$ . Unfortunately, an analytical estimate of  $g$  requires precise knowledge of the shape and disorder of the particle which we lack. A naive estimate of  $g$  in ballistic systems is  $\hbar/\tau d$ , where  $\tau$  is the time for an electron at the Fermi energy to cross the system. The metallic grains of the experiment, however, have a roughly pancake shape. Assuming diffusive dynamics one can show that  $g\tau d/\hbar \propto (z/r)^2$  where  $z$  is the pancake thickness and  $r$  is its radius.  $g$  is therefore much smaller than  $\hbar/\tau d$ .

When  $M$  available states below the highest accessible energy level (including spin), are occupied by  $M' < M$  electrons, there are  $\binom{M}{M'}$  different occupancy configurations. The typical width of a cluster of resonances in this case is  $W^{1/2}cd/g$  where  $W = \min(M - M', M')$ . The width of a cluster of resonances therefore *increases* with the source-drain voltage. The distance between nearby peaks of the cluster, on the other hand, *decreases* as  $W^{1/2}/\binom{M}{M'}$ . This behavior can be seen in Fig. 5.

### 3 Superconducting grains

As illustrated by Fig. 4, the splitting of tunneling resonance peaks in normal metallic grains comes from the possibility of forming different occupation configurations of single-particle states at sufficiently high source-drain voltage. These configurations are reached by resonant tunneling provided relaxation processes are sufficiently slow. This picture also explains the observation that the first cluster in Fig. 2 contains only a single peak. However, the data of Fig. 3 shows that the first peak in the tunneling resonance spectra also splits into several subresonances (see illustration in Fig. 6). This behavior appears when the superconducting grain contains an odd number of electrons and the gate voltage is such that the dot is far from the charge degeneracy point.

In this section we show that the development of a substructure in the first peak of the tunneling resonance spectra is also associated with the generation of nonequilibrium steady state. However in contrast with the resonant tunneling mechanism used in the previous section for the high resonance peaks, here the nonequilibrium steady state is reached by inelastic cotunneling processes.

The principal difference between odd and even grains is that all excitations of the latter are of energy larger than the superconducting gap  $2\Delta$ . Therefore, a source-drain voltage in the range  $V < \Delta/e$  can not induce nonequilibrium states. Odd grains, on the other hand, contain one unpaired electron, which may be shifted to various single-electron levels with characteristic energy scale smaller than the mean level spacing  $d$ . For this reason even a small source-drain voltage  $d < eV < \Delta$  is sufficient to excite the grain. The mechanism of excitation is inelastic cotunneling<sup>13</sup>. Tunneling into the excited grain requires less energetic electrons, and lead in turn to the substructure on the low-voltage shoulder of the of the first resonance, see Figs. 3 and 6. A closely related problem was considered by Averin and Nazarov<sup>14</sup>, however, their theory assumed that relaxation processes prevent the formation of nonequilibrium states. As will be argued in the next section, relaxation processes in ultrasmall metallic grains are very slow, and therefore will be neglected in our theory.

To describe the effect quantitatively, we construct the master equations governing the time evolution of probabilities of different electronic configurations of supercon-



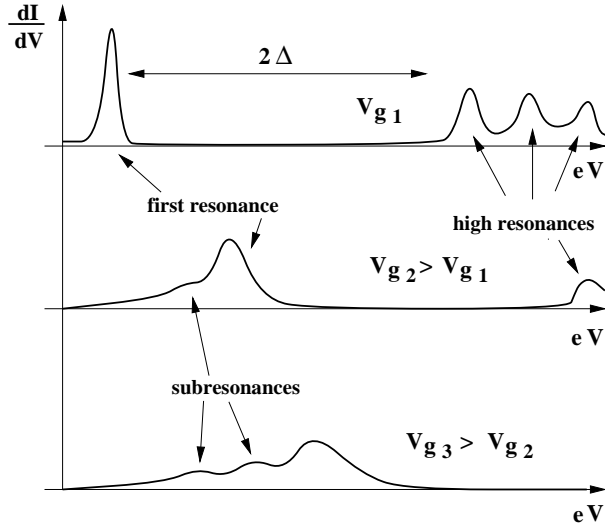


**Figure 6.** A schematic illustration of the differential conductance of an “odd” superconducting grain as function of the source-drain voltage  $V$ , at various gate voltages  $V_g$ . Higher resonances are separated by the superconducting gap from the first one, and subresonances are developed as the first resonance is shifted by the gate voltage.

ducting grains allowing for second order cotunneling processes. The solution of these equations for two limiting cases (one in which two levels participate in the transport, and the other when a large number of levels contribute) explains the substructure of the first peak of the differential conductance illustrated in Fig. 6.

As in the previous section the model Hamiltonian consists of three terms:  $H = H_0 + H_T + H_{\text{int}}$ .  $H_0$ , given by (3), describes the noninteracting electrons in the leads and in the dot;  $H_T$ , given by (4), is the tunneling Hamiltonian, and the interaction Hamiltonian will be approximated by

$$H_{\text{int}} = \frac{e^2}{2C}(N - N_0)^2 - \lambda \sum_{i,j} c_{i\uparrow}^\dagger c_{i\downarrow}^\dagger c_{j\uparrow} c_{j\downarrow}. \quad (5)$$

where  $N = \sum_{j,\sigma} c_{j\sigma}^\dagger c_{j\sigma}$  is the number of electrons in the dot, and  $N_0$  is a continuous parameter controlled by the gate voltage.  $N_0$  determines the finite charging energy required to insert,  $U_+$ , or to remove,  $U_-$ , one electron,

$$U_{\pm} = \frac{e^2}{C} \left[ \frac{1}{2} \pm (N - N_0) \right], \quad |N - N_0| \leq \frac{1}{2}. \quad (6)$$

Consider the experimentally relevant case,  $e^2/C \gg \Delta$ , so that the grain has well defined number of electrons. If this number is even  $N = 2m$ , the ground state energy (we will omit charging part of the energy and restore it later),  $E_{2m} = F_{2m} + 2\mu m$ , can be calculated in the mean field approximation<sup>15, 9</sup> by minimizing thermodynamic potential  $F_{2m} = \sum_k (\xi_k - \epsilon_k) + \Delta^2/\lambda$  where  $\epsilon_k = (\xi_j^2 + \Delta^2)^{1/2}$ , with respect to  $\Delta$ , and by fixing the chemical potential according to the number of electrons in the grain. All the excited states of even dots are separated from the ground state by a large energy,  $2\Delta$ . Considering now the energy spectrum of an odd grain,  $N = 2m - 1$ , we notice that the second term in Eq. (5) operates only within spin singlet states. Therefore, to calculate the low-lying excited states in this case, we fill the single-electron state  $j$  with one electron, and then find the ground state of the remaining  $2m$  electrons with state  $j$  excluded from the Hilbert space. In the mean field approximation it corresponds to the

minimization of the thermodynamic potential  $F_{2m-1}^{(j)} = \sum_{k \neq j} (\xi_k - \epsilon_k) + \Delta^2/\lambda + \xi_j$ . The excited states with energies smaller than  $\Delta$  are characterized by a single index,  $j$  and will be denoted by  $E_{2m-1}^{(j)}$ . In what follows we will need the energy cost of introducing an additional electron into the odd state:  $U_+ + \varepsilon_j$ , where  $\varepsilon_j = E_{2m} - E_{2m-1}^{(j)}$ . In appendix B it is shown that in the limit  $\Delta \gg d$  the result is:

$$\varepsilon_j = \mu_{2m} - \frac{3d}{2} + \frac{\xi_j d}{2\Delta} - \sqrt{\xi_j^2 + \Delta^2}. \quad (7)$$

We turn now to the kinetics of a superconducting grain. Consider the regime where  $U_+ = U \leq \Delta$ ,  $U_- \approx \frac{e^2}{2C} \gg U$ , and  $\frac{e^2}{2C} \gg \Delta \gg d$ . We also assume the conductance of the tunnel barriers to be much smaller than  $e^2/h$ , and that the source-drain voltage is small  $eV < \Delta$ . The simplicity brought to the problem in this regime of parameters stems from the fact that there is only one available state with an even number of electrons (because  $U_- \gg U_+$  one can only add an electron to grain but not subtract one), and whenever the grain contains an even number of electrons it is in its ground state. This imply that even grains cannot be driven out of equilibrium state, while for odd grains tunneling (and cotunneling) takes place via unique state.

Henceforth, we concentrate on grains with an odd ground state. Let us denote by  $P_e$  the probability of finding the grain with an even number of electrons, and by  $P_j$  the probability to find the grain in the odd state  $j$ . Since these states are spin degenerate in the absence of magnetic field,  $P_j$  will denote the sum  $P_{j,\uparrow} + P_{j,\downarrow}$ . The master equations for the probabilities  $P_e, P_j$  have the form

$$\begin{aligned} \frac{dP_e}{dt} &= \sum_j \left[ \Gamma_{o \rightarrow e}^{(j)} P_j - 2\Gamma_{e \rightarrow o}^{(j)} P_e \right], \\ \frac{dP_j}{dt} &= 2 \sum_{i \neq j} [\Gamma_{i \rightarrow j} P_i - \Gamma_{j \rightarrow i} P_j] + 2\Gamma_{e \rightarrow o}^{(j)} P_e - \Gamma_{o \rightarrow e}^{(j)} P_j, \end{aligned} \quad (8)$$

where  $\Gamma_{o \rightarrow e}^{(j)}$  and  $\Gamma_{e \rightarrow o}^{(j)}$  are the transitions rates from the odd  $j$ -th state to the even and from the even to odd respectively, while  $\Gamma_{i \rightarrow j}$  is the rate of transition from the  $i$ -th to the  $j$ -th odd states. Equations (8) are not independent, so they have to be supplied with the normalization condition  $P_e + \sum_j P_j = 1$ . Current in the steady state equals to the electron flow through, say, the left barrier, and for positive  $V$  it is given by

$$I = e \sum_j \left( \Gamma_{o \rightarrow e}^{(j)} + \Gamma_{j \rightarrow j} \right) P_j + 2e \sum_{j \neq i} \Gamma_{j \rightarrow i}^{(j)} P_j. \quad (9)$$

Transition from the  $j$ -th odd state into the even state occurs when  $\mu_L > U + \varepsilon_j$ . The amplitude of this transition is calculated by first order perturbation theory in the tunneling Hamiltonian (4). Fermi's golden rule yields

$$\Gamma_{o \rightarrow e}^{(j)} = g_L \frac{u_j^2 \rho_{Lj} d}{2\pi\hbar} \theta(\mu_L - \varepsilon_j - U), \quad (10)$$

where  $g_L$  is the dimensionless conductance of the left tunnel barrier per one spin,  $u_j = (1 + \xi_j/\epsilon_j)/2$  is the coherence factor,  $\theta(x)$  is the unit step function, and  $\rho_{Lj} = \Omega |\psi_j(r_L)|^2$ , where  $\Omega$  is the volume of the grain and  $\psi_j(r_L)$  is the value of  $j$ -th single-particle wave function at the left point contact  $r_L$ . Energies  $\varepsilon_i$  are given by Eq. (7) and  $U = U_+$  is defined in Eq. (6). Similarly, the rate of transition from even state to  $i$ -th odd state, by tunneling of an electron from the dot to the right lead, is given by

$$\Gamma_{e \rightarrow o}^{(i)} = g_R \frac{v_i^2 \rho_{Ri} d}{2\pi\hbar} \theta(U + \varepsilon_i - \mu_R), \quad (11)$$

where  $g_R$  is the dimensionless conductance of the right tunnel barrier,  $v_i = (1 - \xi_i/\epsilon_i)/2$ , and  $\rho_{Ri} = \Omega|\psi_i(r_R)|^2$ , where  $r_R$  is the position of the right point contact.

A change in the occupation configuration of the odd states occurs via inelastic cotunneling<sup>13</sup>. This mechanism is a virtual process in which an electron tunnels into  $j$ -th available level and another electron tunnels out from the  $i$ -th level. Calculating this rate by second order perturbation theory in the tunneling Hamiltonian, one obtains

$$\Gamma_{j \rightarrow i} = \frac{g_L g_R d^2 u_j^2 v_i^2 \rho_{Lj} \rho_{Ri} (eV - \epsilon_j + \epsilon_i)}{8\pi^3 \hbar (U + \epsilon_j - \mu_L)(U + \epsilon_i - \mu_R)} \quad (12)$$

for  $eV > \epsilon_j - \epsilon_i$ ,  $\mu_L < U + \epsilon_j$ ,  $\mu_R < U + \epsilon_i$ , and zero otherwise.  $\Gamma_{j \rightarrow i}$  diverges in the limits  $\mu_L \rightarrow U + \epsilon_j$  and  $\mu_R \rightarrow U + \epsilon_i$ . It signals that a real transition takes over the virtual one. The region of applicability of Eq. (12) is, therefore,  $U + \epsilon_j - \mu_L > \gamma$  and  $U + \epsilon_i - \mu_R > \gamma$  where  $\gamma \sim gd/4\pi$  is the width of a single-particle level in the dot due to the coupling to the leads,  $g = g_L + g_R$ . However, the interval of biases where Eq. (12) is not valid is narrow, and to the leading approximation in  $\hat{H}_T$  our results will be independent of this broadening.

Let us now apply Eqs. (8) and (9) to describe the appearance of the low-voltage substructure of the first peak. We will consider two situations: (i) small voltage such that only one subresonance can emerge on the shoulder of the leading one, and (ii) large voltage,  $d \ll eV < \Delta$ , where the substructure of the main resonance consists of a large number of subresonances.

In the first case, the chemical potentials of the left and right leads are such that transport through the grain involves only two levels:  $\epsilon_0$  and  $\epsilon_1 < \epsilon_0$  corresponding to the ground and the first excited states of the odd grain. We solve Eqs. (8) for probabilities  $P_0, P_1$  and  $P_e$  using Eqs. (9–12). There are two distinct regimes of the source-drain voltage: (1)  $\mu_L < U + \epsilon_0$  where transport is dominated by cotunneling, and (2)  $\mu_L \geq U + \epsilon_0$  where state “0” is available for resonant tunneling. The substructure of the first resonance in the differential conductance appears in the first regime. Below we show that as  $\mu_L$  passes through  $U + \epsilon_1$ , see Fig. 7, there is a discontinuity in the current-voltage curve. In the first regime, the total current to the leading approximation in  $g_L, g_R$  is a sum of two contributions,  $I \simeq I_{eq} + I_{ne}$ . The first,  $I_{eq} = e\Gamma_{0 \rightarrow 0} + 2e\Gamma_{0 \rightarrow 1}$ , is the equilibrium current coming from cotunneling. The second contribution is associated with the nonequilibrium population of state “1” and is given by

$$I_{ne} = 2e\Gamma_{0 \rightarrow 1} \times \begin{cases} \frac{\Gamma_{1 \rightarrow 0} - \Gamma_{0 \rightarrow 1} + 2\Gamma_{1 \rightarrow 1} - 2\Gamma_{0 \rightarrow 0}}{\Gamma_{0 \rightarrow 1} + \Gamma_{1 \rightarrow 0}} & \mu_L < U + \epsilon_1 \\ 2 \left( 1 + \frac{\Gamma_{e \rightarrow o}^{(1)}}{\Gamma_{e \rightarrow o}^{(0)}} \right) & \mu_L > U + \epsilon_1 \end{cases}$$

Assuming that the voltage drop  $eV = \mu_L - \mu_R$  is larger than the energy difference  $\tilde{d} = \epsilon_0 - \epsilon_1$ , the jump in the nonequilibrium current is:

$$\delta I_{ne} = c_1 e \frac{g_L g_R d^2}{8\pi^2 \hbar \tilde{d}} \left( 1 - \frac{\tilde{d}}{eV} \right) \quad eV \sim 2\tilde{d} \quad (13)$$

where  $c_1 = 4u_0^2 v_1^2 \rho_{L0} \rho_{R1}$  is a constant of order unity. This jump in the nonequilibrium current leads to the peak in the differential conductance spectra. Formula (13) has simple interpretation. Up to numerical prefactors it is a product of two factors: first is the probability of finding the grain with an unpaired electron in state “1”. It is proportional to  $g_R(d/\tilde{d})(1 - \tilde{d}/eV)$ , and increases with the voltage  $V$  and as  $\tilde{d} = \epsilon_0 - \epsilon_1 \rightarrow 0$ . The second factor is associated with the rate in which the state “1” is filled with an electron,  $eg_L d/h$ .

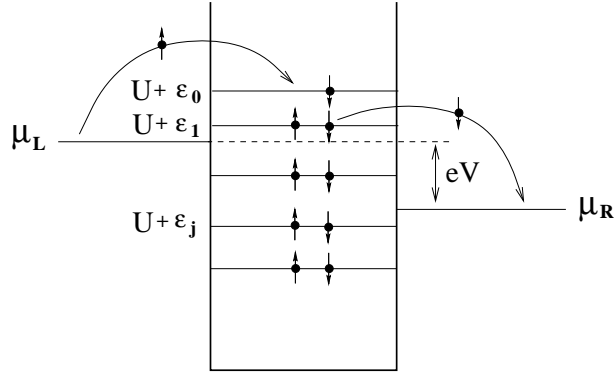


**Figure 7.** Inelastic cotunneling process can drive an “odd” superconducting grain out of its ground state. In the ground state, the single-particle level indicated by  $U + \epsilon_0$  is occupied by one electron. Excited states are those in which the unpaired electron is shifted to other single-particle levels. In a nonequilibrium steady state, low single-particle levels become available for resonant tunneling, leading to a subresonances structure of the differential conductance shown in Fig. 6. State  $j$  shown to be filled with two electrons should be understood as a coherent superposition of double occupied and empty states with weights  $v_j^2$  and  $u_j^2$  respectively.

The magnitude of the jump (13) should be compared to the jump in the current as  $\mu_L$  increases above  $U + \epsilon_0$ , and real transition via the even state become allowed. To the leading order in  $g_L$  and  $g_R$ , the current in this regime is

$$I = c_2 e \frac{g_R g_L d}{h(g_L + 4g_R)}, \quad \mu_L > U + \epsilon_0, \quad (14)$$

where  $c_2$  is a constant of order unity having structure similar to  $c_1$ . Comparing the current jump,  $\delta I_{ne}$ , with that associated with the resonant tunneling,  $\delta I$ , we find

$$\frac{\delta I_{ne}}{\delta I} \simeq \frac{g_L + 4g_R}{8\pi^2}, \quad eV \sim 2\tilde{d}.$$

Thus nonequilibrium population of the excited level of the odd-grain leads to the appearance of a subresonance at small  $V$ , however, its height is much smaller than that of the main resonance.

We turn now to the second regime of the parameters,  $d \ll eV < \Delta$ , in which many levels contribute to the transport. Again, we focus our attention on the cotunneling regime,  $\mu_L < U + \epsilon_0$ . We show that the characteristic amplitude of the subresonances in this regime may become comparable to the amplitude of the main peak.

To the leading order in  $g_L, g_R$ , and  $d/\Delta$ , the steady state solution of the rate equations at  $\mu_L = U + \epsilon_1 + 0$  is  $P_0 \simeq 1$ , while for the other probabilities we have

$$P_e \simeq \frac{\sum_{i \neq 0} \Gamma_{0 \rightarrow i}}{\Gamma_{e \rightarrow 0}^{(0)}}, \quad P_j \simeq 2 \frac{\Gamma_{0 \rightarrow j}}{\Gamma_{o \rightarrow e}^{(j)}} + 2 \frac{\Gamma_{e \rightarrow o}^{(j)}}{\Gamma_{o \rightarrow e}^{(j)}} P_e. \quad (15)$$

The characteristic number of states contributing to the current (9) is large as  $\sqrt{\Delta eV}/d$  so that mesoscopic fluctuations of the tunneling rates and of the inter-level spacings may be neglected. Additional large factor,  $\sqrt{\Delta eV}/d$ , comes from the summation over the levels in Eq. (15), and we find

$$I \simeq \frac{e^2 g_L g_R}{2\pi^2 h} \frac{V \Delta}{\epsilon_0 - \epsilon_j}, \quad \begin{cases} d \ll eV \ll \Delta \\ \mu_L = U + \epsilon_j + 0 \end{cases}.$$

Once again, the current jumps each time  $\mu_L$  passes through  $U + \epsilon_j$ . This jump for large  $j$  (but still such that  $U + \epsilon_j - \mu_L \ll eV$ ) scales as  $1/j^3$ , and the ratio of the jump at  $j = 1$  to the jump at the resonance level (14) is given by

$$\frac{\delta I_{ne}}{\delta I} \simeq \frac{(g_L + 4g_R) eV \Delta}{8\pi^2} \frac{1}{\tilde{d}}, \quad d \ll eV < \Delta.$$

Noticing that  $\tilde{d} = \epsilon_0 - \epsilon_1 \simeq d^2/2\Delta$ , we see that the first subresonance becomes comparable in height to the main one at voltages as small as  $eV \approx 4\pi^2 d^3/\Delta^2 (g_L + 4g_R)$ .

We conclude by comparing the above results with the experimental data of Ref. [6]. There  $\Delta \approx 5d$ , the conductances in the normal state are  $g_R \approx 10g_L \approx 1/8$ , and the leads are also superconducting. The singularity in the density of states of the leads imply that the effective conductance is increased by factor of 2–3. Neglecting inelastic processes and the Josephson coupling, these parameters imply that when  $eV \approx 2d$  the ratio of the subresonances amplitude to that of the first resonance is of order one, while at  $eV \sim 2\tilde{d} \approx d/5$  it is of order of 1%. It implies that first subresonance peak associated with tunneling into state “1” cannot be resolved, both because its amplitude and its distance from the main peak are too small. However next subresonance appear already at distance of order  $d$  from the main resonance, and for  $V > 2d$  have an amplitude comparable with the main resonance.

## 4 Relaxation processes

Central to our analysis is the assumption that the steady-state occupation configurations of the electrons in the dot are far from equilibrium. This condition holds when the rate  $1/\tau_{in}$  of inelastic relaxation processes is smaller than the tunneling rate of an electron into and out of the dot,  $1/\tau_{tun}$ . In the opposite limit,  $1/\tau_{in} > 1/\tau_{tun}$ , the system relaxes to equilibrium between tunneling events, and the electrons effectively occupy only one configuration. In this case one expects each resonance cluster to collapse to a single peak. This behavior is illustrated by the dashed line in Fig. 5 where a large inelastic relaxation rate  $1/\tau_{in} = 5/\tau_{tun}$  was included in the detailed-balance equations.

The data shown in Figs. 2 and 3 indicate that the metal particle in the experimental system is indeed in a strongly nonequilibrium state. It is useful, however, to consider the various relaxation processes in our system in order to delimit the expected nonequilibrium regime. Relaxation of excited Hartree–Fock states may occur due to: (1) electron-electron interaction in the dot beyond Hartree–Fock; (2) electron-phonon interaction; (3) Auger processes in which an electron in the dot relaxes while another one in the lead is excited; (4) relaxation of an electron in the dot as another electron tunnels out to the lead; (5) thermalization with the leads via tunneling. The last two processes are small corrections since they clearly happen on time scales larger than the tunneling time.

In Ref. [16] it was shown that excited many-body states of closed systems with energy  $\epsilon$  smaller than  $(g/\log g)^{1/2}d$  are merely slightly perturbed Hartree–Fock states. In other words, the overlap between the true many-body state and the corresponding Hartree–Fock approximation is very close to unity. This justifies the use of our model for the low energy resonances since  $g \approx 5$  therefore the energy interval  $0 < \epsilon < (g/\log g)^{1/2}d$  contains at least the first few excited states. At high source–drain voltage, however, when the dot is excited to energy  $g^{1/2}d < \epsilon < gd$ , tunneling takes place into quasi-particle states of width  $\epsilon^2/(g^2d)^{17}$ . This width is larger than the typical separation between nearby resonances but smaller than  $d$ . Therefore, electron-electron scattering will obliterate the fine structure of resonances for high energy excitations of the dot.

Consider now the electron–phonon interaction. The temperature, 30 mK, is much smaller than the mean level spacing, therefore, the probability of phonon absorption is negligible, and only emission may take place. The sound velocity in aluminum is  $v_s = 6420$  m/sec, therefore the wavelength of a phonon associated with relaxation of energy  $\omega \sim d = 1$  meV is approximately 50 Å, the same as the system size. In this regime, we estimate the phonon emission rate to be

$$\frac{1}{\tau_{e-ph}} \sim \left(\frac{2}{3}\epsilon_F\right)^2 \frac{\omega^3 \tau d}{2\rho \hbar^4 v_s^5},$$

where  $\epsilon_F$  is the Fermi energy (11.7 eV in Al), and  $\rho$  is the ion mass density (2.7 g/cm<sup>3</sup> in Al). This rate is that of a clean metal but reduced by a factor of  $\tau d/\hbar$  where  $\tau$  is the elastic mean free time<sup>18</sup>. In ballistic systems,  $\tau$  is the traversal time across the system of an electron at the Fermi level. Assuming ballistic motion this factor is of order  $10^{-3}$ . The resulting relaxation rate for  $\omega = d$  is therefore of order  $1/\tau_{e-ph} \approx 10^8$  sec<sup>-1</sup> which is similar to the tunneling rate  $1/\tau_{tun} \approx 6 \cdot 10^8$  sec<sup>-1</sup> (corresponding to a current of  $10^{-10}$  A through the particle). Thus, by increasing the resistance of the tunnel junctions one should be able to cross over to the near-equilibrium regime shown by the dashed line in Fig. 5.

Relaxation due to Auger process is estimated to be negligible. Two factors reduce this rate considerably: (1) it is exponentially small in  $w/\chi$  where  $w$  is the width of the tunnel junction and  $\chi$  is the screening length; (2) interaction between electrons on both sides of the tunnel junction can take place only within a very limited volume.

## 5 Conclusions

In this review it was shown that the low-voltage tunneling-resonance spectra of a ultrasmall metallic grains, normal as well as superconducting, reflect nonequilibrium electron configurations. These configurations are reached by resonant tunneling as well as inelastic cotunneling. The first tunneling resonance develops a substructure on energy scales of order of the single-particle mean level spacing,  $d$ , while high resonances split due to electron-electron interactions and appear in clusters of width  $d/g$ . The latter phenomenon is a result of electron-electron interaction beyond the orthodox model<sup>1</sup>. Relaxation due to electron–phonon interaction, which becomes important for high resistance tunnel barriers, will collapse the clusters. This effect can be used to probe the electron-phonon relaxation rate in nanometer size metal particles.

## Acknowledgments

This review summarize results of collaboration with I. L. Aleiner, B. L. Altshuler, D. C. Ralph, M. Tinkham, and N. S. Wingreen, whom it is my pleasure to thank. I would like also to thank N. Brenner for many useful comments on the manuscript.

## Appendix A

The purpose of this appendix is to calculate the second moment of off-diagonal matrix elements of the interaction potential  $U(\mathbf{r} - \mathbf{r}')$ , and show that  $U_{ijkl}$  are small as  $1/g$ , where  $g$  is the dimensionless conductance. The subject was discussed in several papers,<sup>19, 20, 21</sup> and is presented here for completeness.

When calculating off-diagonal matrix elements of the interaction potential, it is important to take into account screening effects. The relevant two-particle interaction potential is not the bare one,  $\tilde{U}(\mathbf{k})$ , but rather the statically screened potential:  $\tilde{U}_s(\mathbf{k}) = \tilde{U}(\mathbf{k})/[1 + 2\nu\tilde{U}(\mathbf{k})]$  where  $\tilde{U}(\mathbf{k})$  is the Fourier transform of the bare two-particle interaction  $U(\mathbf{r} - \mathbf{r}')$ , and  $\nu$  is the density of states per unit volume. The contribution to the off-diagonal matrix elements comes only from spatial fluctuations in the electron density (non-zero modes) for which screening is established at very short time, of order of the time it takes for a plasmon to propagate through the system. The latter is much shorter than the relaxation time,  $t_c$ , of fluctuations in the electron density. Thus for large  $\nu$  the screened interaction potential,  $U_s(\mathbf{r} - \mathbf{r}')$ , is close to a  $\delta$ -function.

Consider, therefore, the integral

$$U_{ijkl} = \frac{1}{2\nu} \int d\mathbf{r} \psi_i^*(\mathbf{r}) \psi_j^*(\mathbf{r}) \psi_l(\mathbf{r}) \psi_k(\mathbf{r}), \quad (16)$$

where no two indices are the same. Clearly on average  $\langle U_{ijkl} \rangle = 0$  since wave functions associated with different eigenvalues are independent and  $\langle \psi \rangle = 0$ . To estimate the magnitude of the off-diagonal matrix elements we calculate the second moment  $\langle |U_{ijkl}|^2 \rangle$ . The square of the matrix element,  $|U_{ijkl}|^2$ , contains four pairs of wave functions in the form  $\psi_i^*(\mathbf{r}) \psi_i(\mathbf{r}')$ . Since the correlation between wave functions and eigenenergies are only to order  $1/g$ , one can approximate these pairs as

$$\psi_i^*(\mathbf{r}) \psi_i(\mathbf{r}') \approx \frac{d}{2\pi i} [G(\mathbf{r}, \mathbf{r}'; E_i - i\eta) - G(\mathbf{r}, \mathbf{r}'; E_i + i\eta)], \quad (17)$$

where  $d$  is the single-particle mean level spacing,  $\eta$  is a positive energy which will be taken to zero at the end of the calculation, and  $G(\mathbf{r}, \mathbf{r}'; E)$  is the single-particle Green function at energy  $E$ . Two basic correlators emerge when calculating the ensemble or the energy average of  $|U_{ijkl}|^2$ . These correlators, known in disordered diagrammatic nomenclature as the diffuson and Cooperon, are

$$\Pi_\omega(\mathbf{r}, \mathbf{r}') = \langle G(\mathbf{r}, \mathbf{r}'; E + \omega + i\eta) G(\mathbf{r}', \mathbf{r}; E - i\eta) \rangle,$$

and  $\langle G(\mathbf{r}, \mathbf{r}'; E + i\eta) G(\mathbf{r}', \mathbf{r}; E + \omega - i\eta) \rangle$ . For systems with time reversal symmetry, considered here, these correlators are the same. In the semiclassical limit,

$$\Pi_\omega(\mathbf{r}, \mathbf{r}') = 2\pi\nu \sum_\mu \frac{\bar{\chi}_\mu(\mathbf{r}) \chi_\mu(\mathbf{r}')}{-i\omega + \hbar\gamma_\mu}, \quad (18)$$

where the sum is over all classical relaxation modes, i.e. diffusion modes in the case of disordered grains and Perron-Frobenius modes in chaotic systems<sup>§</sup>.  $\gamma_\mu$  are the corresponding eigenvalues, and  $\bar{\chi}_\mu(\mathbf{r})$  [ $\chi_\mu(\mathbf{r}')$ ] is the projection of the Perron-Frobenius left [right] eigenfunctions on the real coordinate space at fixed energy  $E$ .

With the help of (16), (17) and (18), and assuming all energy differences (such as  $E_i - E_j$ ) to be much smaller than  $\hbar\gamma_1$ , one obtains

$$\langle |U_{ijkl}|^2 \rangle \simeq c' \left( \frac{d}{g} \right)^2$$

where  $g = \hbar\gamma_1/d$  is the dimensionless conductance of the system, and  $c'$  is a constant of order unity given by

$$c' = \frac{3}{4\pi^2} \sum_{\mu \neq 0, v \neq 0} \int d\mathbf{r} d\mathbf{r}' \text{Re} \frac{\bar{\chi}_\mu(\mathbf{r}) \chi_\mu(\mathbf{r}')}{\gamma_\mu/\gamma_1} \text{Re} \frac{\bar{\chi}_v(\mathbf{r}') \chi_v(\mathbf{r})}{\gamma_v/\gamma_1}.$$

<sup>§</sup>For simplicity we consider here chaotic systems in the form of billiards, namely the Hamiltonian contains only a kinetic part, and chaotic dynamics is due to the irregular boundary.

Here we assumed for simplicity that  $\gamma_1$  is real. In case it contains also an imaginary part, the same formula applies with the substitution  $\gamma_1 \rightarrow \text{Re}\{\gamma_1\}$ . Notice that there is no zero mode contribution to  $\langle |U_{ijkl}|^2 \rangle$ , since only density fluctuations associated with non zero-modes can induce scattering and contribute to  $U_{ijkl}$ . Mathematically this results from the fact that eigenfunctions,  $\chi_0(\mathbf{r})$  and  $\bar{\chi}_0(\mathbf{r})$ , associated with the zero mode are real, and since  $\Pi_\omega$  is always calculated at a finite energy deference,  $\omega$ , taking its real part excludes the zero-mode contribution.

The rest of this appendix is a semiclassical derivation of formula (18). We begin by writing Green's function in the semiclassical approximation as a sum of two terms<sup>22</sup>:

$$G(\mathbf{r}, \mathbf{r}'; E \pm i\eta) \simeq G_0(\mathbf{r}, \mathbf{r}'; E \pm i\eta) + \sqrt{\frac{2\pi}{h^f \hbar}} \sum_l A_{\mathbf{r}\mathbf{r}',l} e^{\pm \frac{i}{\hbar} S_{\mathbf{r}\mathbf{r}',l}(E)}.$$

Here  $G_0$  is the Weyl contribution associated with “zero length” trajectories. This term is important only at distances  $|\mathbf{r} - \mathbf{r}'|$  of order of the particle wavelength and therefore can be neglected. The second term is a sum over all classical trajectories from  $\mathbf{r}'$  to  $\mathbf{r}$ , in which  $f$  is the number of degrees of freedom,  $S_{\mathbf{r}\mathbf{r}',l}(E)$  is the action, and  $A_{\mathbf{r}\mathbf{r}',l}$  is the corresponding probability amplitude. It is convenient to introduce a local coordinate system in which  $\tau$  is the time along the trajectory, and  $\mathbf{r}_\perp$  are the coordinates perpendicular to the trajectory. In these coordinates<sup>22</sup>

$$|A_{\mathbf{r}\mathbf{r}',l}|^2 = \frac{1}{\dot{r}\dot{r}'} \text{Det}^{-1} \left( \frac{\partial \mathbf{r}_\perp}{\partial \mathbf{p}'_\perp} \right)_l,$$

where  $\dot{r}$  and  $\dot{r}'$  denote the velocity of the particle at the final and initial points, and  $\mathbf{p}'_\perp$  is the conjugate momenta to  $\mathbf{r}'_\perp$ .

Expanding  $S_{\mathbf{r}\mathbf{r}',l}(E + \omega)$  to first order in  $\omega$ , and using the diagonal approximation for the product of the two Green functions, one obtains

$$\Pi_\omega(\mathbf{r}, \mathbf{r}') = \frac{2\pi}{h^f \hbar} \sum_l |A_{\mathbf{r}\mathbf{r}',l}|^2 e^{i\omega T_l/\hbar} = \frac{2\pi}{h^f \hbar} \int dt P(t) e^{i\omega t/\hbar}, \quad (19)$$

where  $T_l = \partial S_{\mathbf{r}\mathbf{r}',l}(E)/\partial E$  is the time associated with the  $l$ -th trajectory, and

$$P(t) = \sum_l \frac{1}{\dot{r}\dot{r}'} \text{Det}^{-1} \left( \frac{\partial \mathbf{r}_\perp}{\partial \mathbf{p}'_\perp} \right)_l \delta(t - T_l). \quad (20)$$

Next we show that  $P(t)$  is the projection of the classical propagator in phase space onto configuration space at fixed energy  $E$ , namely

$$P(t) = \int d\mathbf{p}' \int d\mathbf{p} \delta[E - H(\mathbf{r}, \mathbf{p})] \langle \mathbf{r}, \mathbf{p} | e^{-\mathcal{L}t} | \mathbf{r}', \mathbf{p}' \rangle, \quad (21)$$

where  $H(\mathbf{r}, \mathbf{p})$  is the classical Hamiltonian of the system and  $e^{-\mathcal{L}t}$  is the evolution (Perron-Frobenius) operator for time  $t$ . In the coordinate system introduced above, the Hamiltonian function  $H$  is the conjugate momentum to the time coordinate  $\tau$  along the trajectory, therefore

$$\begin{aligned} P(t) &= \int \frac{dH}{\dot{r}} d\mathbf{p}_\perp \int \frac{dH'}{\dot{r}'} d\mathbf{p}'_\perp \delta(E - H) \delta(H - H'_t) \delta(\tau - \tau'_t) \delta(\mathbf{r}_\perp - \mathbf{r}'_{\perp t}) \delta(\mathbf{p}_\perp - \mathbf{p}'_{\perp t}) \\ &= \frac{1}{\dot{r}\dot{r}'} \sum_l \delta(t - T_l) \int_{\Gamma_l} d\mathbf{p}'_\perp \delta(\mathbf{r}_\perp - \mathbf{r}'_{\perp t}), \end{aligned}$$



where subscript  $t$  denotes the value of the corresponding coordinate after time  $t$  starting from the phase space point  $(\mathbf{r}', \mathbf{p}')$ . Since the energy of the particle is fixed, the integral reduces to a discrete sum over trajectories from  $\mathbf{r}'$  to  $\mathbf{r}$ . The contribution to each trajectory,  $l$ , comes from an infinitesimally small region of the coordinate  $\mathbf{p}'_{\perp}$  denoted by  $\Gamma_l$ . Straightforward integration yields the result (20).

Starting now from (21) and using the spectral decomposition of the Perron-Frobenius operator

$$\langle \mathbf{r}, \mathbf{p} | e^{-\mathcal{L}t} | \mathbf{r}', \mathbf{p}' \rangle = f \delta(p^f - p'^f) \sum_{\mu} e^{-\gamma_{\mu}t} \bar{\varphi}_{\mu}(\mathbf{r}, \mathbf{n}) \varphi_{\mu}(\mathbf{r}', \mathbf{n}'),$$

where  $\mathbf{n}$  denote the direction of the momentum, while  $\bar{\varphi}_{\mu}$  and  $\varphi_{\mu}$  are the left and right eigenfunctions, we get

$$P(t) = h^f \nu \sum_{\mu} e^{-\gamma_{\mu}t} \int \frac{d\mathbf{n}d\mathbf{n}'}{\Omega_f} \bar{\varphi}_{\mu}(\mathbf{r}, \mathbf{n}) \varphi_{\mu}(\mathbf{r}', \mathbf{n}') = h^f \nu \sum_{\mu} e^{-\gamma_{\mu}t} \bar{\chi}_{\mu}(\mathbf{r}) \chi_{\mu}(\mathbf{r}').$$

Here  $\Omega_f = \int d\mathbf{n}$  is the solid angle of a sphere in  $f$  dimensions, and  $\nu = \int d\mathbf{p} \delta(E - H) / h^f$  defines the density of states per unit volume. Substituting this expression in (19) and performing the time integration yields the required result (18).

## Appendix B

In this appendix we derive formula (7) for the cost of introducing an additional electron into an odd state:  $\varepsilon_j = E_{2m} - E_{2m-1}^{(j)}$  (ignoring the charging energy). Denote by  $F_N = E_N - \mu_N N$  the free energy of the system where  $E_N$  is the ground state energy with  $N$  electrons, and  $\mu_N$  is the chemical potential. For the superconducting state with unpaired electron in level  $j$  one has

$$F_{2m-1}^{(j)} = \sum_{k \neq j} (\xi_k - \epsilon_k) + \Delta^2 / \lambda + \xi_j, \quad \epsilon_k = \sqrt{\xi_k^2 + \Delta^2}, \quad (22)$$

where  $\lambda$  is the pairing coupling constant. In the intermediate state where another electron tunneled into the  $j$ -th state and pairs with the already existing one:  $F_{2m} = \sum_k (\xi_k - \epsilon_k) + \Delta^2 / \lambda$ . The parameters in these two equations,  $\Delta$  and  $\mu$  (which are functions of  $N$ ), are determined by the relations:

$$\frac{\partial F_N}{\partial \Delta_N} = 0 \quad N = -\frac{\partial F_N}{\partial \mu_N}$$

Notice that the single-particle energies  $\xi_k$  are measured with respect to the chemical potential, thus for the differentiation with respect to  $\mu_N$  it is convenient to introduce  $\xi_k = \tilde{\xi}_k - \mu_N$ , and  $\epsilon_k = \sqrt{(\tilde{\xi}_k - \mu_N)^2 + \Delta_N^2}$ , where  $\tilde{\xi}_k$  are independent of  $\mu_N$ .

The above derivatives for the *even case*,  $N = 2m$ , give

$$\sum_k \frac{1}{2\sqrt{(\tilde{\xi}_k - \mu_{2m})^2 + \Delta_{2m}^2}} = \frac{1}{\lambda}, \quad 2m = \sum_k \left( 1 - \frac{\tilde{\xi}_k - \mu_{2m}}{\sqrt{(\tilde{\xi}_k - \mu_{2m})^2 + \Delta_{2m}^2}} \right), \quad (23)$$

while for the *odd case*,  $N = 2m - 1$ ,

$$\sum_{k \neq j} \frac{1}{2\sqrt{(\tilde{\xi}_k - \mu_{2m-1}^{(j)})^2 + \Delta_{2m-1}^2}} = \frac{1}{\lambda}, \quad 2m - 2 = \sum_{k \neq j} \left( 1 - \frac{\tilde{\xi}_k - \mu_{2m-1}^{(j)}}{\sqrt{(\tilde{\xi}_k - \mu_{2m-1}^{(j)})^2 + \Delta_{2m-1}^2}} \right). \quad (24)$$

We expand  $\varepsilon_j = E_{2m} - E_{2m-1}^{(j)} = F_{2m}(\mu_{2m}; \Delta_{2m}) - F_{2m-1}^{(j)}(\mu_{2m-1}; \Delta_{2m-1}) + 2m\mu_{2m} - (2m-1)\mu_{2m-1}$  to linear order in the differences  $\Delta_{2m} - \Delta_{2m-1}$ , and  $\mu_{2m} - \mu_{2m-1}$ :

$$\begin{aligned}\varepsilon_j &\simeq F_{2m}(\mu_{2m}; \Delta_{2m}) - F_{2m-1}(\mu_{2m}; \Delta_{2m}) + \mu_{2m} \\ &= \mu_{2m-1}^{(j)} - \sqrt{(\tilde{\xi}_j - \mu_{2m})^2 + \Delta_{2m}^2}.\end{aligned}\quad (25)$$

We are left, now, with the problem of finding the dependence of  $\mu_{2m-1}^{(j)}$  on the unpaired electron state  $j$ . For this purpose we choose  $\mu_{2m}$  as the reference point and calculate the difference  $\mu_{2m-1}^{(j)} - \mu_{2m}$ . From Eqs. (23) and (24) we have

$$\begin{aligned}2m-2 &= \sum_{k \neq j} \left( 1 - \frac{\tilde{\xi}_k - \mu_{2m-1}^{(j)}}{\sqrt{(\tilde{\xi}_k - \mu_{2m-1}^{(j)})^2 + \Delta_{2m-1}^2}} \right) \\ &= \sum_k \left( 1 - \frac{\tilde{\xi}_k - \mu_{2m}}{\sqrt{(\tilde{\xi}_k - \mu_{2m})^2 + \Delta_{2m}^2}} \right) - \left( 1 - \frac{\tilde{\xi}_j - \mu_{2m}}{\sqrt{(\tilde{\xi}_j - \mu_{2m})^2 + \Delta_{2m}^2}} \right) \\ &\quad - (\mu_{2m-1}^{(j)} - \mu_{2m}) \sum_k \left( \frac{-1}{\sqrt{(\tilde{\xi}_k - \mu_{2m})^2 + \Delta_{2m}^2}} + \frac{(\tilde{\xi}_k - \mu_{2m})^2}{((\tilde{\xi}_k - \mu_{2m})^2 + \Delta_{2m}^2)^{3/2}} \right).\end{aligned}$$

(The correction to  $\Delta$  vanishes in the limit where the single-particle mean level spacing  $d$  is much smaller than the superconducting gap,  $d \ll \Delta$ ). Since the first sum in the second line equals  $2m$  we have

$$\begin{aligned}-2 &= 1 - \frac{\tilde{\xi}_j - \mu_{2m}}{\sqrt{(\tilde{\xi}_j - \mu_{2m})^2 + \Delta_{2m}^2}} + \sum_k \frac{(\mu_{2m-1}^{(j)} - \mu_{2m})\Delta_{2m}^2}{((\tilde{\xi}_k - \mu_{2m})^2 + \Delta_{2m}^2)^{3/2}} \\ &\simeq 1 - \frac{\tilde{\xi}_j - \mu_{2m}}{\Delta} + (\mu_{2m-1}^{(j)} - \mu_{2m}) \int \frac{d\xi}{d} \frac{\Delta^2}{(\xi^2 + \Delta^2)^{3/2}}.\end{aligned}$$

Thus

$$\mu_{2m} \simeq \mu_{2m-1}^{(j)} + \frac{d}{2} \left( 3 - \frac{\xi_j}{\Delta} \right),$$

and substituting this result in (25) we obtain (7).

## REFERENCES

1. D. V. Averin and K. K. Likharev, in *Mesoscopic Phenomena in Solids*, eds. B. L. Altshuler, P. A. Lee, and R. A. Webb (Elsevier, NY, 1991) pp. 173–271.
2. M. Kastner, *Rev. Mod. Phys.*, **64**, 849 (1992).
3. D.V. Averin and A.N. Korotkov, *Sov. Phys. JETP*. **97**, 1161 (1990).
4. A.T. Johnson *et. al.*, *Phys. Rev. Lett.* **69**, 1592 (1992); S. Tarucha *et. al.*, *ibid.*, **77**, 3613 (1996).
5. D.C. Ralph, C.T. Black, and M. Tinkham, *Physica B* **218**, 258 (1996).
6. D.C. Ralph, C.T. Black and M. Tinkham, *Phys. Rev. Lett* **78**, 4087 (1997).
7. O. Agam, N. S. Wingreen, B. L. Altshuler, D. C. Ralph, and M. Tinkham, *Phys. Rev. Lett.*, **78**, 1956 (1997).
8. O. Agam and I. L. Aleiner, *Phys. Rev. B*, **56**, R5759 (1997).
9. J. von Delft, A. D. Zaikin, D. S. Golubev, and W. Tichy *Phys. Rev. Lett.* **77**, 3189 (1996) ; R. A. Smith and V. Ambegaokar, *Phys. Rev. Lett.* **77**, 4962 (1996).
10. D. V. Averin and A. N. Korotkov, *Zh. Eksp. Teor. Fiz.* **97**, 1661 (1990) [*Sov. Phys. JETP* **70**, 937 (1990)]. This work neglects fluctuations of the interaction energy ( $\delta U=0$ ).

11. Ya. M. Blanter, A. D. Mirlin and B. A. Muzykanskii, Phys. Rev. Lett. **78** 2449 (1997).
12. O. Agam, B. L. Altshuler, and A. V. Andreev, Phys. Rev. Lett. **75**, 4389 (1995).
13. D.V. Averin and A.A. Odintsov, Phys. Lett. A **140**, 251 (1990); D.V. Averin and Yu.N. Nazarov, Phys. Rev. Lett. **65**, 2446 (1990).
14. D.V. Averin and Yu.N. Nazarov, Phys. Rev. Lett. **68**, 1993 (1992).
15. M. Tinkham, *Introduction to superconductivity*, (McGraw–Hill, New York, 1980).
16. B. L. Altshuler, Y. Gefen, A. Kamenev, and L. S. Levitov, Phys. Rev. Lett. **78**, 2803 (1997).
17. U. Sivan, Y. Imry, and A. G. Aronov, Europhys. Lett. **28**, 115 (1994).
18. M. Yu Reizer and A. V. Sergeev, Zh. Eksp. Teor. Fiz. **90**, 1056 (1986) [Sov. Phys. JETP **63**, 616 (1986)].
19. Ya. M. Blanter, Phys. Rev. B **54**, 12807 (1996).
20. Ya. M. Blanter and A. D. Mirlin, Phys. Rev. E **55**, 6514 (1997).
21. I. L. Aleiner and L. I. Glazman, cond-mat/9710195 (1997).
22. M. C. Gutzwiller, *Chaos in Classical and Quantum Mechanics* (Springer, New York, 1990).